

Combined micro computed tomography and histology study of bone augmentation and distraction osteogenesis

Bernd Ilgenstein^a, Hans Deyhle^a, Claude Jaquier^b, Christoph Kunz^b, Anja Stalder^a,
Stefan Stübinger^c, Gernot Jundt^b, Felix Beckmann^d, Bert Müller^a, and Simone Elke Hieber^{*a}

^aBiomaterials Science Center, University of Basel, c/o University Hospital, 4031 Basel, Switzerland;

^bUniversity Hospital Basel, 4031 Basel, Switzerland;

^cCompetence Center for Applied Biotechnology and Molecular Medicine (CABMM),
Musculoskeletal Research Unit, University of Zurich, 8057 Zurich, Switzerland;

^dInstitute of Materials Research, Helmholtz-Zentrum Geesthacht, 21502 Geesthacht, Germany

ABSTRACT

Bone augmentation is a vital part of surgical interventions of the oral and maxillofacial area including dental implantology. Prior to implant placement, sufficient bone volume is needed to reduce the risk of peri-implantitis. While augmentation using harvested autologous bone is still considered as gold standard, many surgeons prefer bone substitutes to reduce operation time and to avoid donor site morbidity. To assess the osteogenic efficacy of commercially available augmentation materials we analyzed drill cores extracted before implant insertion. In younger patients, distraction osteogenesis is successfully applied to correct craniofacial deformities through targeted bone formation. To study the influence of mesenchymal stem cells on bone regeneration during distraction osteogenesis, human mesenchymal stem cells were injected into the distraction gap of nude rat mandibles immediately after osteotomy. The distraction was performed over eleven days to reach a distraction gap of 6 mm. Both the rat mandibles and the drill cores were scanned using synchrotron radiation-based micro computed tomography. The three-dimensional data were manually registered and compared with corresponding two-dimensional histological sections to assess bone regeneration and its morphology. The analysis of the rat mandibles indicates that bone formation is enhanced by mesenchymal stem cells injected before distraction. The bone substitutes yielded a wide range of bone volume and degree of resorption. The volume fraction of the newly formed bone was determined to 34.4% in the computed tomography dataset for the augmentation material Geistlich Bio-Oss[®]. The combination of computed tomography and histology allowed a complementary assessment for both bone augmentation and distraction osteogenesis.

Keywords: Dentistry, dental implant, bone graft, bone microstructure, bone morphology, dental biopsies, human mesenchymal stem cells, hematoxylin and eosin stain

1. INTRODUCTION

Successful osseointegration of dental implants depends on the sufficient availability of healthy bone. Frequently, local bone defects result from tooth extraction or pathological defects like periodontal disease, cysts, granuloma, tumor or trauma. After healing, a vertical and horizontal bone deficit can be assessed and has to be grafted [1-3]. For smaller bone defects insertion of an implant combined with bone augmentation using an osteoconductive material is the current standard procedure [4, 5]. In cases of larger defects, a two stage surgical procedure is favored to insure primary stability of the implant immediately after implantation. The surgical procedure includes the bone harvesting at a donor region and the insertion at the defect site. The usage of autologous bone is still the gold standard for bone augmentation, but harvesting bone from intra- and/or extra-oral donor sites remains a critical procedure and induces considerable morbidity. The most frequently used substitutes are xenografts and alloplastic materials. Synthetic or allogenic materials are also favored by many patients. Detailed studies about integration of augmented autologous bone or osteoconductive materials, based on histology and micro computed tomography, are still rare. Such studies support the decision of patient and oral surgeon on the selection of the most appropriate bone augmentation procedure including commercially available augmentation materials. Because suppliers often provide augmentation materials and dental implants together, these studies can have major influence on this important market.

*E-mail: simone.hieber@unibas.ch, phone: +41 61 265 9118, Fax: +41 61 265 9699, www.bmc.unibas.ch

To avoid bone harvesting, distraction osteogenesis can be performed. Even though the implant survival rate for distraction osteogenesis shows promising results (94.7%) [6], it is still a technique with limitations such as unidirectional movement of the bone, advanced surgical training, patient compliance, and significant complications associated with failure [7]. Distraction osteogenesis proved to be a powerful tool for correcting craniofacial deformities, especially in younger patients [8]. The simultaneous expansion of the bone and the surrounding soft tissue promises an enhancement of further growth and stability. The time effort is a main drawback of the procedure resulting in high costs and the risk of disturbed healing during the consolidation period. Therefore, the current challenges are the increase of the distraction rate and the acceleration of osseous consolidation while preserving the quality of the newly formed bone [8, 9]. Qi *et al.* [10] showed that mineralization of the distracted callus can be enhanced by injecting stem cells after distraction. The hypothesis that stem cells in the distraction inter-zone are necessary during the distraction protocol has been tested by distracting mandibles of nude rats with and without stem cell injection. Within this context, the question of how the performance of the distraction protocol can be quantitatively determined arises.

Histology is an established method to judge the healing process in hard tissues [11-15] and yields functional information. The disadvantages of the approach are the significant effort for serial sectioning and the restricted spatial resolution in the third dimension. Therefore, micro computed tomography (μ CT) is complementary to histology in acquiring the three-dimensional (3D) morphology of bony tissues. For example, it has been successfully applied to assess the bone quality after augmentation with bone substitutes [4]. Bone phases with different degrees of mineralization were distinguished based on the measured X-ray absorption values. The method also allows for the quantitative evaluation of bone formation around bone implants [16, 17].

Therefore, we have evaluated the osteogenic efficacy of three commercially available augmentation materials by analyzing drill cores taken before the implant insertion. A direct comparison of the materials is highly desirable in order to select the most promising material for the individual patient as already mentioned above. In the present study we assess the potential of a combined analysis based on both hard X-ray micro computed tomography (μ CT) and histology to determine the quality of newly formed bone for augmentation materials and distraction osteogenesis.

2. MATERIALS AND METHODS

2.1 Surgical procedures using augmentation substitutes

In all cases the surgical concept was a two-stage therapy. The operations were carried out under local anesthetic (Lidocain epinephrine Streuli, Streuli Pharma, Switzerland) on the patients. First, mid-crestal incision with lateral mucoperiosteal flap reflection allowed the identification of the bone volume and the desired implant position. Due to a lack of bone, an augmentation operation was performed with autologous bone, different substitutes or a defined mixture of autologous bone with a substitute. For the augmentation therapy substitutes of established suppliers, i.e. Geistlich Bio-Oss[®] (Geistlich Pharma AG, Wolhusen, Switzerland), BoneCeramic[™] (Straumann, Basel, Switzerland), and easy-graft[™] (Degradable Solutions AG, Schlieren, Switzerland) were used. In all cases the augmentation material in the augmented region was covered with a resorbable membrane (Remotis[®], Thommen Medical AG, Waldenburg, Switzerland/ Geistlich Bio-Gide[®], Geistlich Pharma AG, Baden-Baden, Germany). After periosteal relieving incision the wound was closed with non-resorbable sutures. For the alveolar ridge preservation, easy-graft[™] (Degradable Solutions AG, Schlieren, Switzerland) was used. The insertion of implants was performed after a bone-healing period of six months on average. The re-entry was performed in the same region as the bone augmentation and the specimens were taken at the planned area of the dental implant. The dental implant was only inserted in satisfactory conditions of the newly formed bone.

Figure 1 shows the surgical procedure. After the termination of the bone-healing period and before implant insertion, bone biopsies were extracted using a hollow drill with an inner diameter of 2 mm and 3 mm, depending on the implant diameter. Immediately after the surgery, the harvested bone specimens were carefully removed from the drill and transferred to 4% formalin solution for fixation. The specimens were stored in this solution until embedding (see below) or until beamtime at the synchrotron radiation sources was available. This procedure has no negative effect on the patient, but allows collection of bone specimens directly from the implantation site.

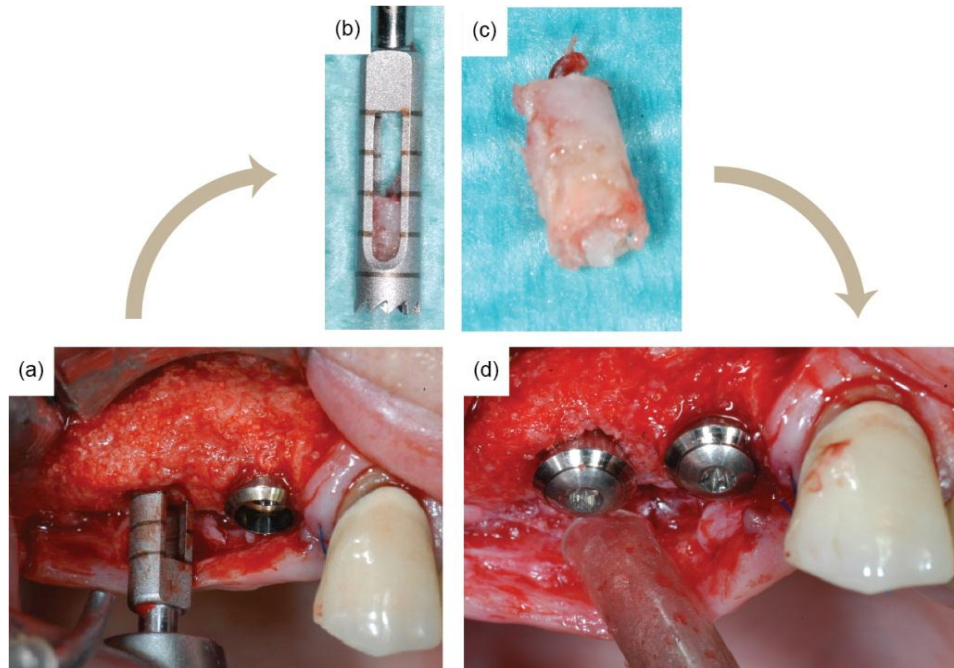


Figure 1. Procedure to harvest specimens: (a) trepan boring tool creating the hole for the implant, (b) hollow drill filled with specimen, (c) specimen harvested, (d) clinical situation after implant placement.

2.2 Distraction osteogenesis

The effect of human mesenchymal stem cells (hMSC) applied at the beginning of the distraction protocol has been studied on nude rats (Protocol approval No. 2295, cantonal veterinary office, Basel, Switzerland). After a latency period of five days, linear distraction was performed at a rate of 0.5 mm per day up to a distraction distance as large as 6 mm. A total of four animals (two with hMSCs) were included in this preliminary study. Briefly, animals were anesthetized by inhalation using a mixture of isoflurane (1.5% to 3.0%) and oxygen (0.6 l/min). After shaving and disinfection, the mandible was exposed at the area of the angle. The specially designed rat mandible distractor (AO Development Institute, Davos, Switzerland) was fixed onto the mandible using pins about 1 mm in diameter. After this preparation, the osteotomy of the mandible was performed using a piezo surgery tool, which selectively cuts bone and protects soft tissue. In two animals hMSCs were injected within the distraction gap after re-suspending the cells in fibrin glue (Baxter, Vienna, Austria), reference animals were treated with fibrin glue only. The skin was closed using resorbable sutures. Post-operatively, buprenorphine was administered every 12 h for 48 to 72 h (0.01 to 0.05 mg/kg). After a latency period of five days the distractor was moved anteriorly once a day for the duration of 11 d (regular distraction), or for the duration of 4 days (rapid distraction) to reach a 6 mm distraction gap. For this short manipulation animals were anesthetized by inhalation. After the consolidation period (regular distraction: 72 days, rapid distraction: 66 days), animals were sacrificed by inhalation of carbon dioxide. The mandibles were carefully harvested for the further evaluation using μ CT and histology.

2.3 Micro computed tomography

Synchrotron radiation-based micro computed tomography (SR μ CT) measurements of the bone substitutes were performed at the beamline W 2 (HASYLAB at DESY, Hamburg, Germany) operated by the HZG-Research Center, Geesthacht, Germany, in standard absorption contrast mode [18]. The specimens were measured at 25 keV photon energy and 2.2 μ m pixel size. 721 equidistant projections were acquired over 180°. The data were reconstructed using a standard filtered back-projection algorithm available at the beamline. Before reconstruction, the projections were binned by a factor of four to increase density resolution [19] and reduce the size of the dataset for ease of handling. The spatial resolution was derived from the 10% value of the modulation transfer function obtained from imaging a highly X-ray absorbing metal edge [20] and corresponded to values between 3.0 and 4.2 μ m.

The scanning of the distraction specimens was carried out with a phoenix nanotom[®] s scanner (GE Measurement and Control, Wunstorf, Germany). The nanotom[®] is a 160-kV nanofocus CT scanner, equipped with a 5-megapixel

(2304 × 2304 pixels) CCD detector and is capable of achieving a minimum pixel size of less than 0.5 μm. The scanner could accommodate the entire jaw with a maximal length of 16 mm. The data acquisition was performed at an acceleration voltage of 100 kVp and a beam current of 100 μA. The 2000 projections were scanned over 360° with an exposure time of 0.5 s per frame, resulting in a total scan duration of approximately 100 minutes per specimen. The magnification was chosen so that the entire specimen fitted into the field of view leading to a pixel size 6.9 μm. The 3D reconstruction was performed by the nanotom[®] producer's software (phoenix datos|x), based on a modified Feldkamp algorithm, with a correction to reduce ring artifacts and beam hardening. The resulting 3D dataset consists of 16-bit values relating to the local X-ray density.

After de-calcification, selected rat mandibles were scanned at the beamline BW 2 (HASYLAB at DESY, Hamburg, Germany) [18] operated by the HZG Research Center. SRμCT-measurements in absorption contrast mode were performed using an asymmetric rotation axis [16] and photon energy of 14 keV. The magnification was set to 1.76, which led to a pixel size of 2.5 μm and a spatial resolution of 9.4 μm derived from the 10% value of the modulation transfer function from a highly X-ray absorbing metal edge [20]. The 1440 projections recorded at equidistant angular positions between -180° and 180° were reconstructed using a filtered back-projection algorithm and were binned by a factor of two before reconstruction to increase density resolution [19].

2.4 Histology

The embedded bone biopsies were placed in a special polytetrafluoroethylene mold and embedded with a methymethacrylate solution consisting of methacrylatacid-methylester (Sigma-Aldrich Chemie GmbH, Buchs, Switzerland), dibutylphtalate (Merck-Schuchardt OHG, Hohenbrunn, Germany) and perkadox (Dr. Grogg Chemie AG, Stetten, Switzerland) in a proportion of 89.5 : 10.0 : 0.5. To ensure a vertical position of the sample axis during the polymerization process the specimens were stabilized with cured methacrylate blocks from the same solution. After embedding they were stored and dried at room temperature. To cut 300 μm-thin sections for histology, a diamond saw (Leica 1 SP 1600, Leica Instruments GmbH, Nussloch, Germany) was used.

The sections were glued (Cementit[®] CA 12, Merz+Benteli AG, Niederwangen, Switzerland) on opal acrylic slides (Perspex[®] GS Acrylglas Opal 1013, Wachendorf AG, Basel, Switzerland), wrapped in aluminum foil and pressed overnight under a metal block of 1 kg weight.

Further thinning of the slices was achieved through grinding (EXAKT 400 CS, EXAKT Apparatebau GmbH, Norderstedt, Germany) with sandpaper (grit size 1200, Struers GmbH, Birmensdorf, Switzerland) until the target thickness was reached. Subsequently, the surfaces were polished on a Struers Planopol-V (Struers GmbH, Birmensdorf, Switzerland) with sandpaper (grit size 4000, Struers GmbH, Birmensdorf, Switzerland). The polished sections were etched with formic acid (methanoic acid, 0.7%, Sigma-Aldrich Chemie GmbH, Buchs, Switzerland) for two minutes, cleaned and etched for another two minutes, rinsed with water and later surface stained with toluidine blue (1% stock solution in 0.1 M phosphate buffer pH 8.0, Sigma-Aldrich Chemie GmbH, Buchs, Switzerland) for ten minutes. The sections were digitally recorded with a microscope (Leica M420, Camera DFC 320, Leica Microsystems, Heerbrugg, Switzerland, magnification 1.0 × 18.6-22.3) using the software Image Manager 1000 (Leica Microsystems, Heerbrugg, Switzerland).

The specimens of the rat mandible were embedded into paraffin and cut into 2 μm-thin sections using a sliding microtome (Leica SM2010R, Leica Instruments GmbH, Nussloch, Germany). The sections were stained with hematoxylin and eosin (H&E) stain.

3. RESULTS

3.1 Augmentation materials

Figure 2 shows a bone specimen eight months after alveolar ridge preservation. A canine tooth in the aesthetic area was removed and the socket was filled to avoid bone resorption. The synthetic substitute consists of individual tri-calcium phosphate-hydroxyapatite (TCP/HA) granules fused together by a poly-lactic-glycolic acid layer that covers each granule. The coated granules appear inhomogeneous due to variations in X-ray absorption and are represented in light grey to white. The resolution of the SRμCT data enables a clear visualization of the granules and of the newly formed bone in-between. Dark grey-colored bony tissue can be identified between the granules. Thus, it is expected that the bone is clinically stabile, which is important for the preservation of local bone structures after tooth extraction and, finally, for the successful osseointegration of the dental implant. The rather qualitative view onto the three orthogonal slices is

translated to quantities using the X-ray absorption histogram (cp. Figure 2). It allows for the identification of the components based on their X-ray absorption. The main peak above zero absorption originates from the PMMA embedding and is almost black in the three slices. The comparison of the slices and the histogram verifies that the peak at the X-ray absorption of around 4 cm^{-1} relates to the newly formed bone. The bone augmentation material does not produce a well-defined peak, as its inhomogeneous composition and density lead to a wide variety of X-ray absorption values.

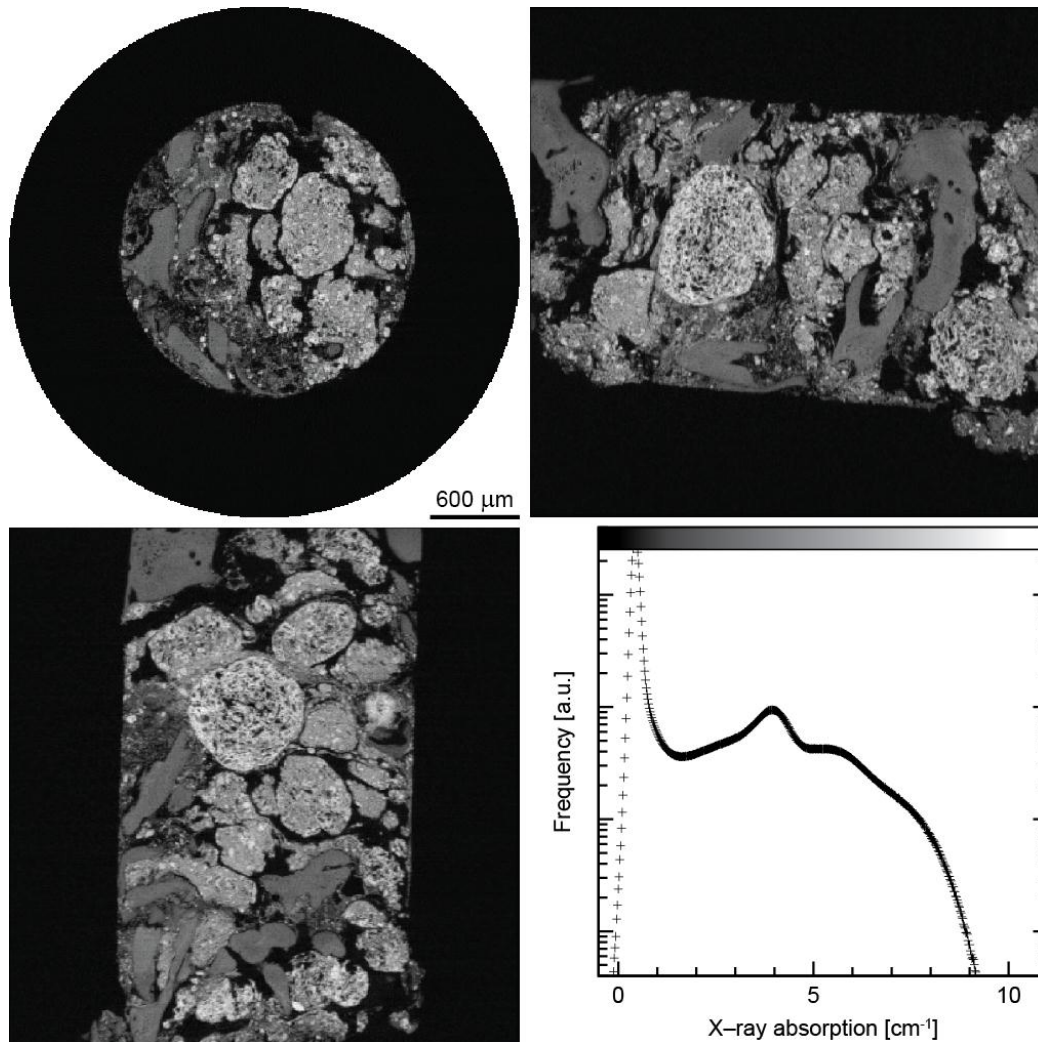


Figure 2. Three orthogonal slices through specimen easy-graft™ (Degradable Solutions AG, Schlieren, Switzerland) and the corresponding absorption histogram. Newly formed bone is shown in dark gray, restoration material in light gray to white. Structures in medium gray correspond to restoration material, which is being resorbed and transformed into endogenous bone.

Figure 3 shows a bone specimen harvested from the molar alveolar region, which was augmented with BoneCeramic™ (Straumann AG, Basel, Switzerland). Bone augmentation material and bone can be easily distinguished by the differences in X-ray absorption. Only a small amount of augmentation material is present in the specimen, indicating that most of it might have been resorbed and substituted with bone. The amount of augmentation material present after specimen harvesting can be quantified using the X-ray absorption histogram. One can easily count the voxels with a local X-ray absorption larger than 6 cm^{-1} . The peak's maximum at absorption values of 10 cm^{-1} has a shoulder to smaller values because of partial volume phenomena. Bone in different maturation stages could be distinguished. Higher mineralized bone appears brighter due to the higher X-ray absorption. It is generally surrounded by

younger bone, which also exhibits a higher degree of micro-porosity. Inside the larger voids, material exhibiting rather low X-ray absorption can be identified. This fact cannot only be derived from the slices, but also from the absorption histogram (cp. Figure 3), which contains numerous peaks. Each peak can be related to bone with a different degree of mineralization and/or density. The peak at the X-ray absorption of about 2 cm^{-1} , however, is rather attributed to partial volume phenomena between the main bone peak at absorption values of around 4 cm^{-1} and the embedding material PMMA with absorption values close to zero.

From a clinical point of view, it is expected that the area from which the specimen has been harvested is sufficiently regenerated for implant insertion.

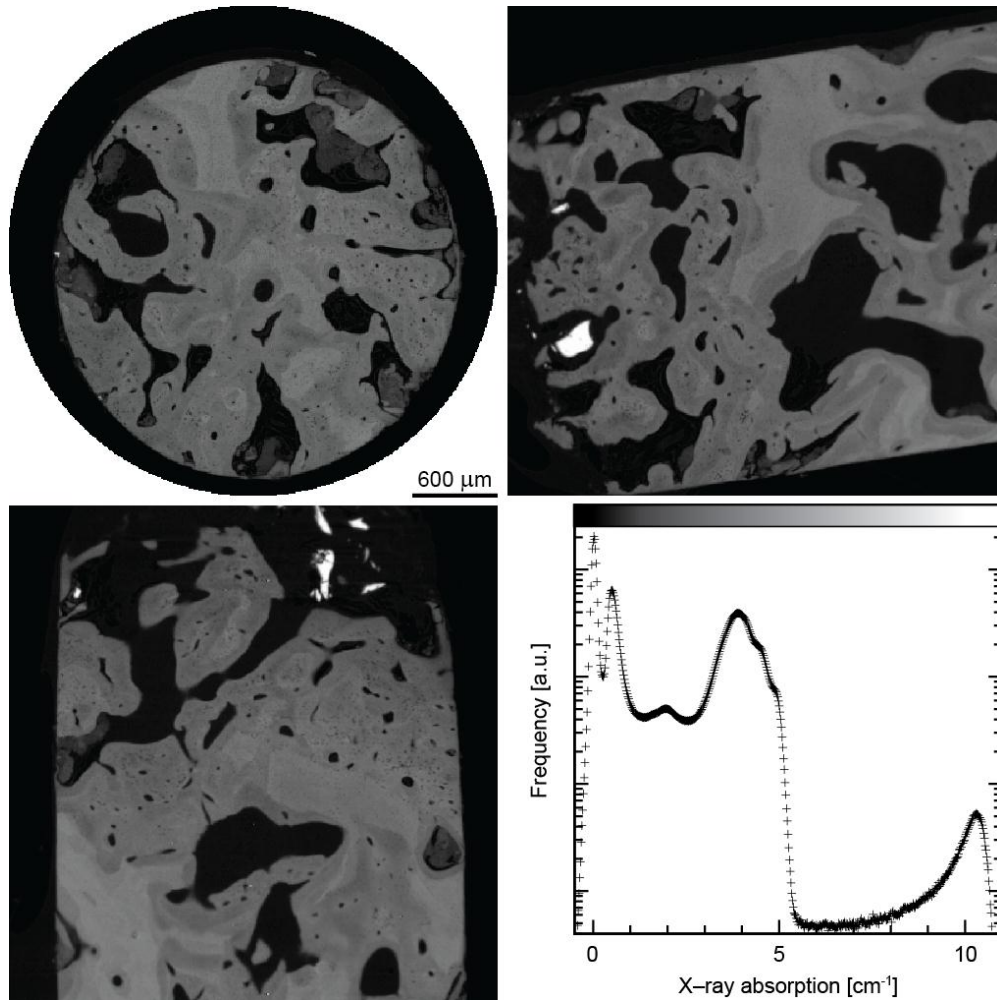


Figure 3. Three orthogonal slices through specimen BoneCeramic™ (Straumann, Basel, Switzerland) and the corresponding absorption histogram. Only a few augmentation material particles (represented in white) are present in the specimen, indicating that most of it has been resorbed and substituted with bone.

Figure 4 shows a specimen harvested from a sinus lift augmentation in the molar region, performed with Geistlich Bio-Oss® (Geistlich Pharma AG, Wolhusen, Switzerland). This situation is of particular interest, because originally no autologous bone is present in the region of the augmentation, which is located above the palate. Only a thin layer of bone is present below the augmented bone. As a result, the border between the newly formed hard tissue and the autologous bone can be identified as a plane perpendicular to the main axis of the harvested cylinder. Based on the absorption values, cp. images and histogram, autologous and newly formed bone can be segmented using a simple intensity-based tool (thresholding). Here, the threshold of about 4 cm^{-1} can be applied. Further thresholds can be applied to segment the other components, i. e. air – peak close to zero absorption, embedding material (PMMA) – peak at the absorption values of about 0.8 cm^{-1} and augmentation material – peak at absorption values between 6 and 8 cm^{-1} .

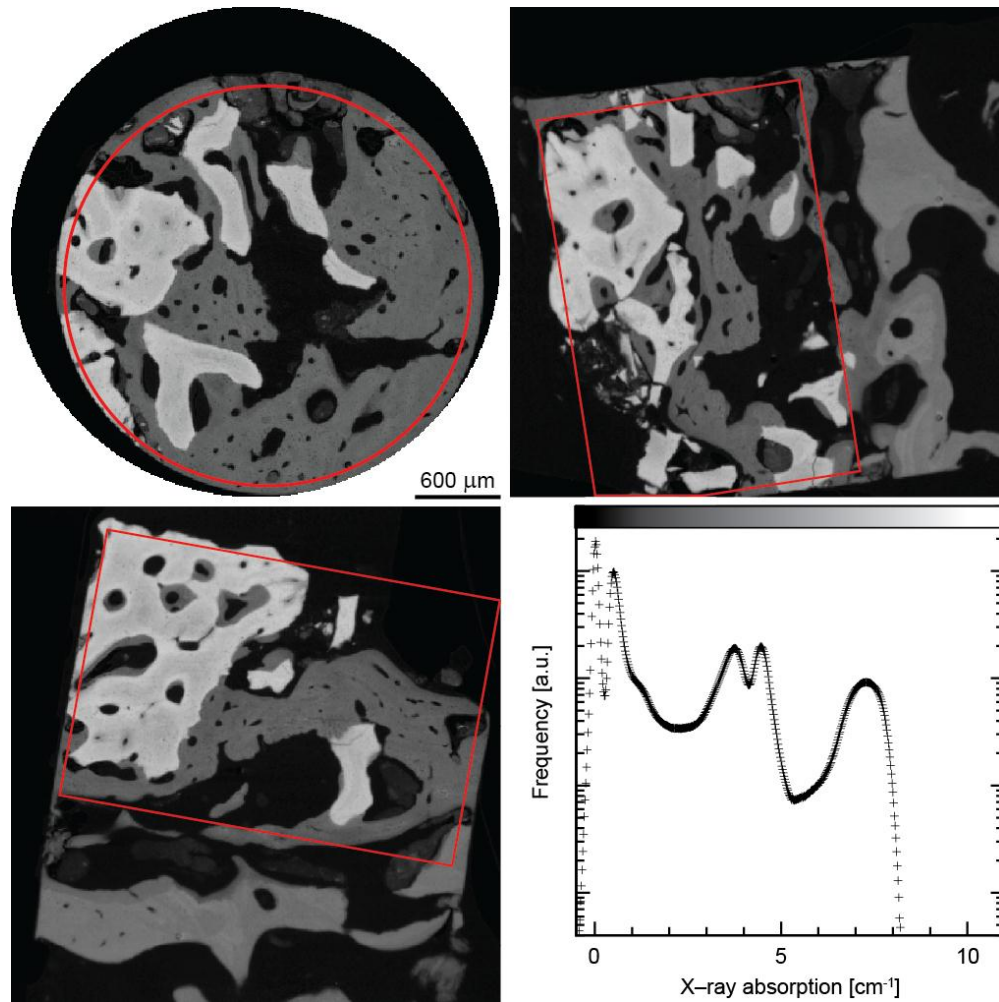


Figure 4. Three orthogonal cuts through specimen Geistlich BioOss® (Geistlich Pharma AG, Wolhusen, Switzerland) and the corresponding absorption histogram of the tomography data. Newly formed bone can be seen in dark gray, restoration material in light gray/white and autologous bone in medium gray. The region outlined in red was extracted for bone volume determination (see below).

To determine the amount of newly formed bone, a cylindrical region of interest (ROI) could be virtually cut from the sinus lift specimen, corresponding to the region given in Figure 4 using the red-colored lines. This selected ROI, represented in Figure 5, is completely located in the augmented region to avoid preparation artifacts that could be present at the cylindrical surface. It is smaller than the harvested specimen, but still large enough to determine a meaningful value for the volume of newly formed bone. It corresponds to 34.4% of the ROI.

The results of the segmentation are displayed in Figure 5. Thresholds are set to the minima between the peaks in the absorption histogram. The voxels with a local X-ray absorption below about 2 cm^{-1} were set transparent, such that air and embedding material are invisible. The voxels with absorption values between 2 and 4 cm^{-1} are represented by light gray and correspond to the newly formed bone. The autologous bone with local X-ray absorption values between 4 and 5 cm^{-1} is given in darker gray. The augmentation material present after the regeneration exhibits X-ray absorption values that are above 5 cm^{-1} and are displayed in red color.

The different components can be virtually extracted from the tomography data to examine them individually, see Figure 5. For example, medical experts can evaluate the morphology by having a look from different viewing angles.

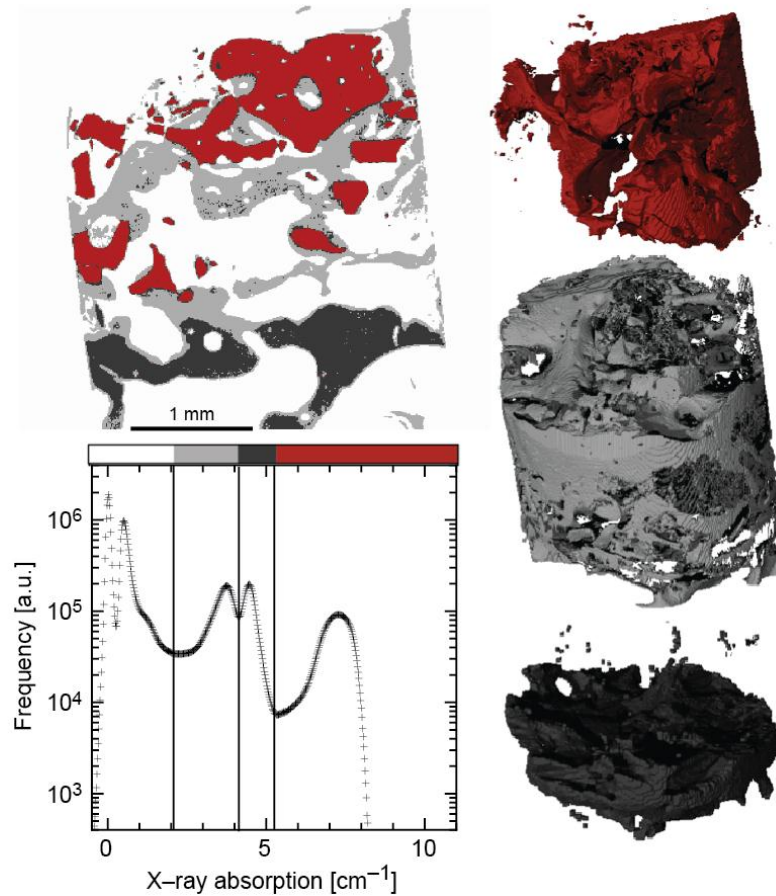


Figure 5. On the left, vertical slice through the specimen from the sinuslift restored by a xenograft material (Geistlich Bio-Oss®, Geistlich Pharma AG, Wolhusen, Switzerland). The components of the specimen, namely restoration material (red), newly formed bone (light gray) and autologous bone (dark gray) can be segmented by thresholding, as shown in the absorption histogram. On the right, the segmented components are rendered in 3D.

Figure 6 compares a 10 μm -thin histological slice of the specimen prepared using BoneCeramic™ (Straumann AG, Basel, Switzerland) with the corresponding μCT -slice represented in similar colors. Bone appearing in dark blue in the histological slice (left) is also represented in blue in the related μCT -slice (right). Discrepancies in shape in the lower part originate from preparation artifacts during histology. The histology of such specimens is demanding because of the different mechanical properties of the components, namely bone and augmentation material. Therefore, artifacts including tissue deformations, cracks and missing parts, are commonly present. The variations in color brightness result from the varying degree of calcification. Toluidine blue staining allows a differentiation between mature, calcified bone (light blue) and new bone formation (dark blue). In addition to the calcified bony tissues, parts of the residual tissue (e.g. soft tissue) or artifacts (e.g. fixation glue) were also stained by toluidine blue. They do not correspond to calcified tissue, because they are not recognizable in the μCT data. Bone substitutes shown in the μCT in white are not found in the histology data. The material was lost during the preparation procedure.

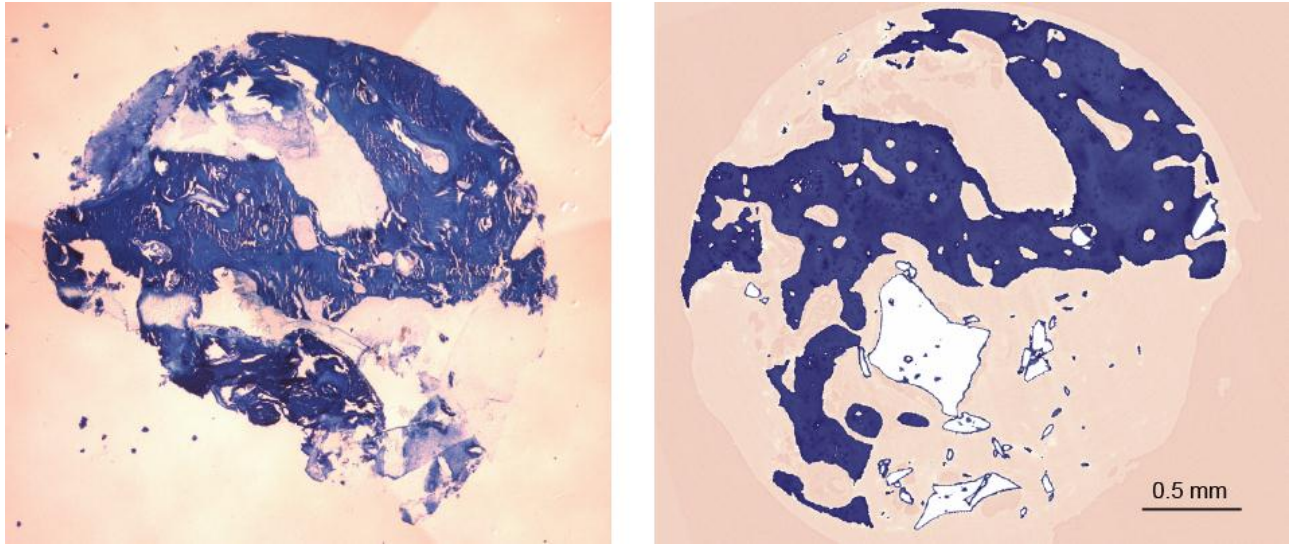


Figure 6. Comparison of a histological slice (left) and the corresponding slice of the SR μ CT dataset given in similar colors (right) for the bone augmentation using BoneCeramic™ (Straumann AG, Basel Switzerland). In the histological section, highly calcified bone shows up in dark blue, less calcified bone in light blue. The restoration material represented in white in the SR μ CT dataset is missing in the histological slice.

3.2 Distraction osteogenesis

The distracted specimens were initially analyzed using the nanotom[®] s. After de-calcification, SR μ CT were performed from the same specimen. The reconstructions as shown in Figure 7 reveal the 3D morphology and internal bone structure. The newly formed bone features a similar X-ray absorption to the original bone. Thus it cannot be segmented using thresholding. The borders of the distraction region, however, feature sharp edges at the exterior geometry. They are a result of the initial cut in the mature bone before distraction. The rat mandible distracted under the presence of additional hMSC shows a considerable amount of newly formed bone, whereas in the other specimen the distraction gap collapsed due to the lack of bone formed.

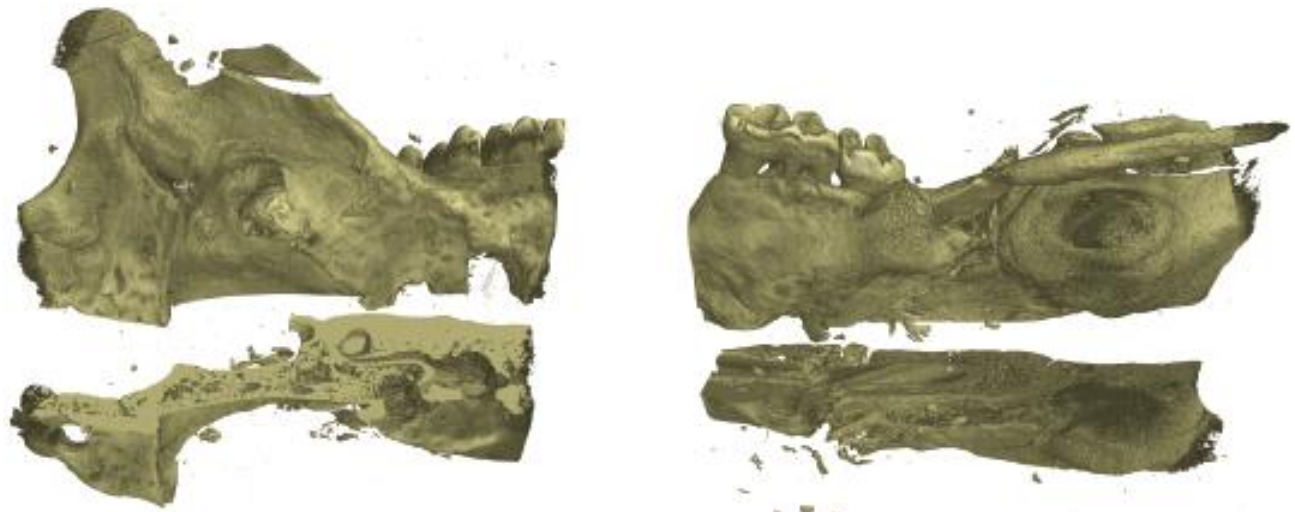


Figure 7. 3D representations of the mandibles after regular distraction with injection of stem cells (left) and without injecting hMSC (right) scanned by the nanotom[®] s before de-calcification. The virtual cuts show representative cross-sections of the interior. Complete osseous bridging of the distraction gap is observed with hMSC, whereas osseous healing remains incomplete in the other case.

Figure 8 compares the de-calcified rat mandibles measured in SR μ CT scans and their histological slices. The SR μ CT-data were used to identify and localize the most interesting cross-sections for the histological cuts. The dominant features in the histological slices, i.e. bone, teeth, muscles (Figure 8 right) can also be recognized in the cross-sections of the 3D data (Figure 8 left). The borders between the original and the newly formed bone can be identified by the characteristics of the osteotomy site, i. e. sharp edges of the outer bone, enclosing the distraction region. Bridging the distraction region was only achieved by the injection of hMSC as already noticeable in the nanotom[®]- μ CT scans (Figure 7).

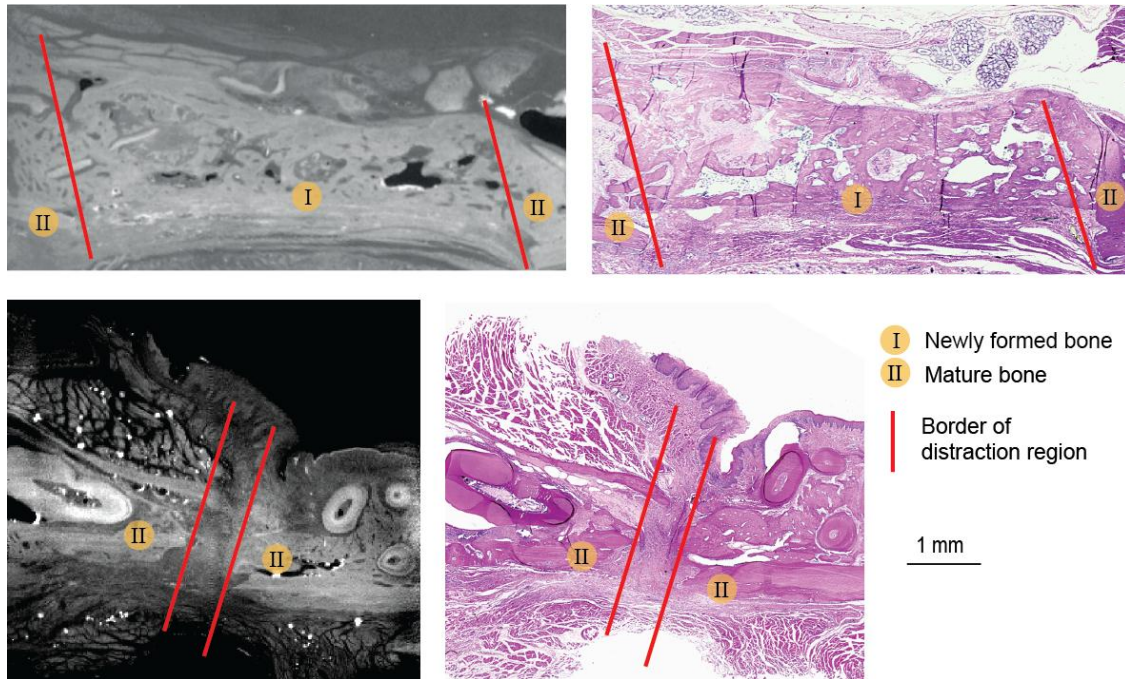


Figure 8. Cross-sections of the SR μ CT data (left) and the corresponding histological slices with H&E staining (right) of the mandibles after distraction with injection of stem cells (top) and without injected hMSC (bottom). The area between the red lines corresponds to the distraction region. The histology confirms that the distraction osteogenesis using hMSC leads to a complete bridging between the osteotomy sites, whereas the bone healing in the reference animal.

4. DISCUSSION

The reconstruction of bone defects before implant insertion is a frequent necessity when bone is lost after extraction therapy or when pathological bone defects were present. Within this context, the usage of synthetic materials as bone substitutions is considered as an alternative to reconstruction with autologous human bone and has to be evaluated in detail. Classically, assessments of the bone quality have been performed by histology. In histology, the cellular structures including osteoblasts and osteoclasts, i. e. the bone surface, can be identified. The information, however, is restricted to 2D space and in the third dimension even using serial sectioning the resolution is limited to the order of 10 μ m.

Therefore, SR μ CT is an efficient technique to evaluate the bone quality after augmentation with bone substitutes [4]. Compared to conventional, X-ray tube-based systems SR μ CT delivers improved density resolution because of the constant photon energy and allows for a more precise quantification of bone density (degree of mineralization). Bone phases with different degrees of mineralization can be segmented based on their absorption values. The high spatial and density resolution in SR μ CT, however, comes to the cost of high delivered doses. Therefore, *in vivo* measurements as know from dentistry [21] are impossible. In the present study, bone specimens harvested after bone augmentation were analyzed by SR μ CT to image the hard tissues and the remaining augmentation materials. SR μ CT, although well suited for hard tissue imaging, does hardly permit differentiation between soft tissues, especially in specimens where also bone is present. Histology, however, helps to identify the soft tissue types via staining. The present study shows preliminary data of selected histology and SR μ CT-slices to correlate the features identified.

The combination of CT-methods and histology enables us not only to evaluate the maturation and mineralization of the bone, but also the clear identification of cellular structures using histology [13]. The 2D information as represented by the histological sections can then be extrapolated to the 3D features [4].

In the data of our preliminary study, one finds a variation in bone volume and degree of resorption. The bone substitute we used for socket preservation (easy-graft™) showed stable clinical conditions. Based on clinical experience the material is recommended for alveolar ridge augmentation. Different opinions concerning the effect of alveolar ridge preservation (ARP) exist. It was claimed that ARP is still necessary, although the success might be limited. The application of bone grafts does not always promote the formation of bone. Hovarth *et al.* discussed the value of ARP in detail and concluded that the resorption of the alveolar ridges cannot be totally prevented [22]. Serino *et al.* found significantly higher trabecular bone volumes after the application of ARP [23]. The calcium phosphates showed biocompatibility properties and are, therefore, suited for bone graft substitute materials [24]. The SRμCT data of the easy-graft™-treated specimens showed areas of substitute resorption and regeneration with newly formed bone, whereas the solution of the coating polymer layers was incomplete. This might be one reason why the clinical experience differs from the common interpretation of radiological data.

The specimen from the bone augmentation using BoneCeramic™ showed a complete regeneration of the treated areas. Only small amounts of remaining augmentation materials were detected after a healing period of six months. The SRμCT data revealed a well-defined region of newly formed bone with different phases, characterized by distinctive degrees of mineralization.

Xenograft biomaterials such as Geistlich BioOss® that consist of HA from bovine bone have scaffolding properties. They are poorly resorbed for a long period of time [5, 25]. In the present study we have found that the augmentation material was well integrated. Only some parts of the augmentation material were not surrounded by newly formed bone, which indicates osteoconductivity properties.

Within this context, it has to be noted that the small number of specimens incorporated into the presented study does not allow for a clinically relevant evaluation of the augmentation materials.

Among the different specimen processing methods tested for histology we have realized that a thin sectioning of the methacrylate-embedded specimens is less suitable due to the brittleness of the HA components. As a result, the HA components were lost in the sections. Therefore, we decided to prepare thick sections [26]. Choosing this approach we lost valuable parts of the specimen through sawing and grinding. Here, the non-destructive nature of SRμCT is a major advantage.

In the case of distraction osteogenesis, both histology and CT-analysis are non-trivial methods to assess the quality of the newly formed bone. The manual inspection of the histological slices is well established, but time-consuming and expensive. CT offers a non-destructive analysis based on 3D data. Sato *et al.* already used μCT to quantify the newly formed bone between the bone surface and a distraction plate [27]. Here, the identification of distractions was rather simple because of the geometry of the set up. The CT assessment revealed an enhancement by stem cell injection in rabbits. In the present study, the distraction region could be identified by the morphological changes at the border from mature to newly formed bone before and after de-calcification. The scans of both conventional μCT and SRμCT revealed a bridging of the mandible bone when stem cells were injected before distraction. The osseous bridging was missing in the case without stem cell injection. The SRμCT dataset after de-calcification additionally allowed the detailed analysis of the inner zone in the distraction region and the identification of soft tissue components, complementary to the histological analysis. Moreover, the radiological assessment was very helpful to localize the interesting regions within the specimen and the necessary sliding directions.

5. CONCLUSIONS

The combination of synchrotron radiation-based micro computed tomography and selected histological sections provides a detailed quantitative view of both bone morphology and maturation. The SRμCT-data provides details about the bone morphology in 3D but does not allow for the identification of non-calcified bone as is possible in histological slices. Bone cells such as osteoblasts and osteoclasts are not directly accessible using current X-ray-based methods because of their size and because they only yield absorption values, which may overlap with other features such as connective tissue or the embedding material. The functional staining in histology, however, allows visualization of cells. The information

from the 2D histological sections can be used to interpret features within the 3D CT-data. This is helpful, since the isotropic voxels of the features can be counted for quantifications including the determination of newly formed bone. Additionally, the tomograms can be used to determine the slices of interest in any direction of the specimens for histological sectioning. As a result, SR μ CT and histological methods are complementary tools to assess the bone, which is formed after the application of augmentation materials or hMSC-supported distraction osteogenesis.

In summary, μ CT is a powerful method to evaluate the 3D structure of bone down to the cellular level [28]. It also allows a characterization of augmentation materials [29]. Most interesting from a clinical point of view is the interface between biomaterial and tissue. This preliminary study demonstrates that this interface is accessible even in cases of complex morphology.

ACKNOWLEDGMENTS

The authors would like to thank Nunzia Di Maggio (Tissue Engineering, University of Basel) for the preparation of the stem cells. Beamtime was granted through the project proposals I-20110780 EC and I-20110555 EC (HASYLAB at DESY, Hamburg, Germany).

REFERENCES

- [1] Barone, A., Aldini, N. N., Fini, M., Giardino, R., Calvo Guirado, J. L., and Covani, U., "Xenograft versus extraction alone for ridge preservation after tooth removal: A clinical and histomorphometric study," *J. Periodontol.* 79(8), 1370-1377 (2008).
- [2] Buser, D., von Arx, T., ten Bruggenkate, C., and Weingart, D., "Basic surgical principles with ITI implants," *Clin. Oral Implants Res.* 11(1), 59-68 (2000).
- [3] Schropp, L., Wenzel, A., Kostopoulos, L., and Karring, T., "Bone healing and soft tissue contour changes following single-tooth extraction: a clinical and radiographic 12-month prospective study," *Int. J. Periodont. Rest.* 23(4), 313-323 (2003).
- [4] Bernhardt, R., Scharnweber, D., Müller, B., Beckmann, F., Göbbels, J., Jansen, J., Schliephake, H., and Worch, H., "3D analysis of bone formation around titanium implants using micro computed tomography (μ CT)," *Proc. SPIE* 6318, 631807 (2006).
- [5] Zitzmann, N. U., Scharer, P., Marinello, C. P., Schüpbach, P., and Berglund, T., "Alveolar ridge augmentation with Bio-Oss: A histologic study in humans," *Int. J. Periodont. Rest.* 21, 289-295 (2001).
- [6] Aghaloo, T. L., and Moy, P. K., "Which hard tissue augmentation techniques are the most successful in furnishing bony support for implant placement?," *Int. J. Oral. Max. Impl.* 22, 49-70 (2007).
- [7] Fiorellini, J. P., and Nevins, M. L., "Localized ridge augmentation/preservation. A systematic review," *Ann. Periodontol.* 8(1), 321-327 (2003).
- [8] Kunz, C., Adolphs, N., Buescher, P., Hammer, B., and Rahn, B., "Distraction osteogenesis of the canine mandible: the impact of acute callus manipulation on vascularization and early bone formation," *J. Oral Maxil. Surg.* 63(1), 93-102 (2005).
- [9] Jaquier, C., Schaeren, S., Farhadi, J., Mainil-Varlet, P., Kunz, C., Zeilhofer, H. F., Heberer, M., and Martin, I., "In vitro osteogenic differentiation and in vivo bone-forming capacity of human isogenic jaw periosteal cells and bone marrow stromal cells," *Ann. Surg.* 242(6), 859-868 (2005).
- [10] Qi, M., Hu, J., Zou, S., Zhou, H., and Han, L., "Mandibular distraction osteogenesis enhanced by bone marrow mesenchymal stem cells in rats," *J. Cranio. Maxill. Surg.* 34(5), 283-289 (2006).
- [11] Bataille, R., Chappard, D., Alexandre, C., Dessauw, P., and Sany, J., "Importance of quantitative histology of bone changes in monoclonal gammopathy," *Br. J. Cancer* 53(6), 805-810 (1986).
- [12] Brownfield, L. A., and Weltman, R. L., "Ridge preservation with or without an osteoinductive allograft: A clinical, radiographic, micro-computed tomography, and histologic study evaluating dimensional changes and new bone formation of the alveolar ridge," *J. Periodontol.* 83(5), 581-589 (2012).

- [13] Hedberg, E. L., Kroese-Deutman, H. C., Shih, C. K., Lemoine, J. J., Liebschner, M. A. K., Miller, M. J., Yasko, A. W., Crowther, R. S., Carney, D. H., Mikos, A. G., and Jansen, J. A., "Methods: A comparative analysis of radiography, microcomputed tomography, and histology for bone tissue engineering," *Tissue Eng.* 11(9), 1356-1357 (2005).
- [14] Kennedy, D. W., Senior, B. A., Gannon, F. H., Montone, K. T., Hwang, P., and Lanza, D. C., "Histology and histomorphometry of ethmoid bone in chronic rhinosinusitis," *Laryngoscope* 108(4), 502-507 (1998).
- [15] Ullmark, G., and Orbrant, K. J., "Histology of impacted bone-graft incorporation," *J. Arthroplasty* 17(2), 150-157 (2002).
- [16] Müller, B., Bernhardt, R., Weitkamp, T., Beckmann, F., Bräuer, R., Schurigt, U., Schrott-Fischer, A., Glückert, R., Ney, M., Beleites, T., Jolly, C., and Schamweber, D., "Morphology of bony tissues and implants uncovered by high-resolution tomographic imaging," *Int. J. Mat. Res.* 98(7), 613-621 (2007).
- [17] Bernhardt, R., Scharnweber, D., Müller, B., Thurner, P., Schliephake, H., Wyss, P., Beckmann, F., Göbbels, J., and Worch, H., "Comparison of microfocus- and synchrotron X-ray tomography for the analysis of osteointegration around Ti6Al4V implants," *Eur. Cells Mater.* 7, 42-51 (2004).
- [18] Beckmann, F., Herzen, J., Haibel, A., Müller, B., and Schreyer, A., "High density resolution in synchrotron-radiation-based attenuation-contrast microtomography," *Proc. SPIE* 7078, 70781D (2008).
- [19] Thurner, P., Beckmann, F., and Müller, B., "An optimization procedure for spatial and density resolution in hard X-ray micro-computed tomography," *Nucl. Instrum. Meth. B* 225, 599-603 (2004).
- [20] Müller, B., Thurner, P., Beckmann, F., Weitkamp, T., Rau, C., Bernhardt, R., Karamuk, E., Eckert, L., Buchloh, S., and Wintermantel, E., "Non-destructive three-dimensional evaluation of biocompatible materials by microtomography using synchrotron radiation," *Proc. SPIE* 4503, 178-188 (2002).
- [21] Dalstra, M., Cattaneo, P. M., and Beckmann, F., "Synchrotron radiation-based microtomography of alveolar support tissues," *Orthod. Craniofac. Res.* 9(4), 199-205 (2006).
- [22] Horváth, A., Mardas, N., Mezzomo, L. A., Needleman, I. G., and Donos, N., "Alveolar ridge preservation. A systematic review.," *Clin. Oral Invest.* in press, (2012).
- [23] Serino, G., Rao, W., Iezzi, G., and Piattelli, A., "Polylactide and polyglycolide sponge used in human extraction sockets: bone formation following 3 months after its application," *Clin. Oral Implants Res.* 19(1), 26-31 (2008).
- [24] Schmidlin, P. R., Nicholls, F., Kruse, A., Zwahlen, R. A., and Weber, F. E., "Evaluation of moldable, in situ hardening calcium phosphate bone graft substitutes," *Clin. Oral Implants Res.*, in press (2012).
- [25] Araujo, M. G., and Lindhe, J., "Ridge preservation with the use of Bio-Oss collagen: A 6-month study in the dog," *Clin. Oral. Implants Res.* 20(5), 433-440 (2009).
- [26] Holmes, R. E., and Hagler, H. K., "Porous hydroxylapatite as a bone graft substitute in mandibular contour augmentation: A histometric study," *J. Oral Maxil. Surg.* 45(5), 421-429 (1987).
- [27] Sato, K., Haruyama, N., Shimizu, Y., Hara, J., and Kawamura, H., "Osteogenesis by gradually expanding the interface between bone surface and periosteum enhanced by bone marrow stem cell administration in rabbits," *Oral Surg. Oral Med. O* 110(1), 32-40 (2010).
- [28] Peyrin, F., Dong, P., Pacureanu, A., Zuluaga, M. A., Olivier, C., Langer, M., and Cloetens, P., "Synchrotron radiation CT from the micro to nanoscale for the investigation of bone tissue," *Proc. SPIE* 8506, (2012).
- [29] Maspero, F. A., Ruffieux, K., Müller, B., and Wintermantel, E., "Resorbable defect analog PLGA scaffolds using CO₂ as solvent: structural characterization," *J Biomed. Mater. Res.* 62(1), 89-98 (2002).